



EN



Dergi Listesi

Dergi Adı

ISSN

Yıl

Temizle

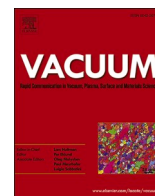
Ara

No	Yıl	Dergi Adı	ISSN	Çeyreklik Grup	Katsayı	kategori	Dergi Puanı
103618	2021	VACUUM	0042-207X	Q2	0.8	SCIE	

Sayfada 10 Kayıt Göster

Önce

1 Kayıttan 1 - 1 Arası Kayıtlar



In-situ and ex-situ face-to-face annealing of epitaxial AlN

Merve Nur Koçak^{a,c}, Kağan Murat Pürlü^a, İzel Perkitel^{a,b}, İsmail Altuntaş^{a,b}, İlkey Demir^{a,b,*}

^a Nanophotonics Research and Application Center, Sivas Cumhuriyet University, 58140, Sivas, Turkey

^b Department of Nanotechnology Engineering, Faculty of Engineering, Sivas Cumhuriyet University, 58140, Sivas, Turkey

^c Department of Metallurgical & Materials Engineering, Faculty of Engineering, Sivas Cumhuriyet University, 58140, Sivas, Turkey

ARTICLE INFO

Keywords:

AlN
MOVPE
RTA
Face-to-face annealing

ABSTRACT

AlN films have been deposited on c-plane sapphire substrates by metalorganic-vapor-phase-epitaxy (MOVPE). The changes in the film structure have been investigated by applying different annealing processes which are ex-situ rapid thermal annealing (RTA) and in-situ process after the nucleation-layer (NL). The AlN nucleation-layer grown on sapphire has been annealed face-to-face with ex-situ (RTA) process for 3 min and with in-situ process for 3 h, then pulsed-atomic-layer-epitaxy AlN film has been grown at a high temperature. The samples have been characterized by high-resolution X-ray diffraction, atomic force microscopy, Ultraviolet–visible spectrometry, and Raman scattering to examine the structural properties, surface morphology, and optical properties. The sample annealed with the ex-situ (RTA) process, where rapid diffusion took place, has reached larger grain sizes and the dislocation density has decreased as the grain boundary decreased. Although better crystal quality has been obtained with the ex-situ (RTA) process, it has been observed that the surface roughness of the sample annealed with the ex-situ (RTA) process is higher than that of the sample annealed with the in-situ process. Considering the results, a schematic prediction of the growth process after face-to-face annealing has been proposed. Experimental findings have shown that different annealing processes after growing the AlN-NL have a great effect on the properties of the AlN.

1. Introduction

In recent years, III-N group materials have been preferred in electronic and optoelectronic devices such as light-emitting diodes (LEDs), laser diodes (LDs), high electron mobility transistors (HEMTs), high power p-n diodes, and Schottky diodes [1–5]. AlN, which is a member of the III-N group, is thought as a material of the near future due to its unique properties such as large band gap (6.2 eV), high critical electric field (450 kV/cm), high thermal conductivity (590 W/mK), and high-temperature stability. AlN is typically used as a buffer layer to obtain GaN-based devices with low-defect density [6]. Moreover, it is a candidate material to replace substrates such as sapphire, Si, and SiC, which are widely used for nitride-based electronic and optoelectronic applications. A lot of research has been carried out on the growth and characterization of AlN thin films to show the advantages of this material. Many different growth methods have been used to grow AlN films such as chemical vapor deposition (CVD), molecular beam epitaxy (MBE), pulsed sputter deposition (PSD), pulsed laser deposition (PLD), hydride vapor phase epitaxy (HVPE), reactive magnetron, and MOVPE [7–10]. CVD is one of the suitable techniques to control preferred

orientation. The pulsed sputter deposition method is handy for the growth of high-quality AlN films at room temperature, but the obtained films by this technique have significant residual compressive stress. PLD includes molten tiny particles or target parts in deposited films, which decrease the quality of the films. High-quality AlN films can be obtained with MBE, but it is not appropriate for thick films owing to the slow growth rate. The HVPE method has a high growth rate, but it results in high defect density in the grown films. It is thought that the MOVPE is one of the most effective growing methods due to its high growth rate, high-quality yield, high production capacity, and low cost.

AlN epitaxial films are usually grown as heteroepitaxy and the sapphire is widely used as a preferred substrate for AlN growth owing to its easy availability and low cost. Low mobility of Al adatoms, the parasitic reaction between sources, the lattice mismatch, and thermal expansion co-efficient mismatches between sapphire and AlN are some of the challenges encountered in growing high-quality AlN thin films. In the literature, many different approaches have been used to obtain a high-quality AlN structure on a sapphire substrate; changing the Al/N ratio for the AlN-NL, high growth temperature, two-stage growth, and epitaxial lateral overgrowth (ELOG), etc. [11–14]. It has been reported

* Corresponding author. Nanophotonics Research and Application Center, Sivas Cumhuriyet University, 58140, Sivas, Turkey.

E-mail address: idemir@cumhuriyet.edu.tr (İ. Demir).

<https://doi.org/10.1016/j.vacuum.2022.111284>

Received 1 April 2022; Received in revised form 18 June 2022; Accepted 18 June 2022

Available online 26 June 2022

0042-207X/© 2022 Elsevier Ltd. All rights reserved.

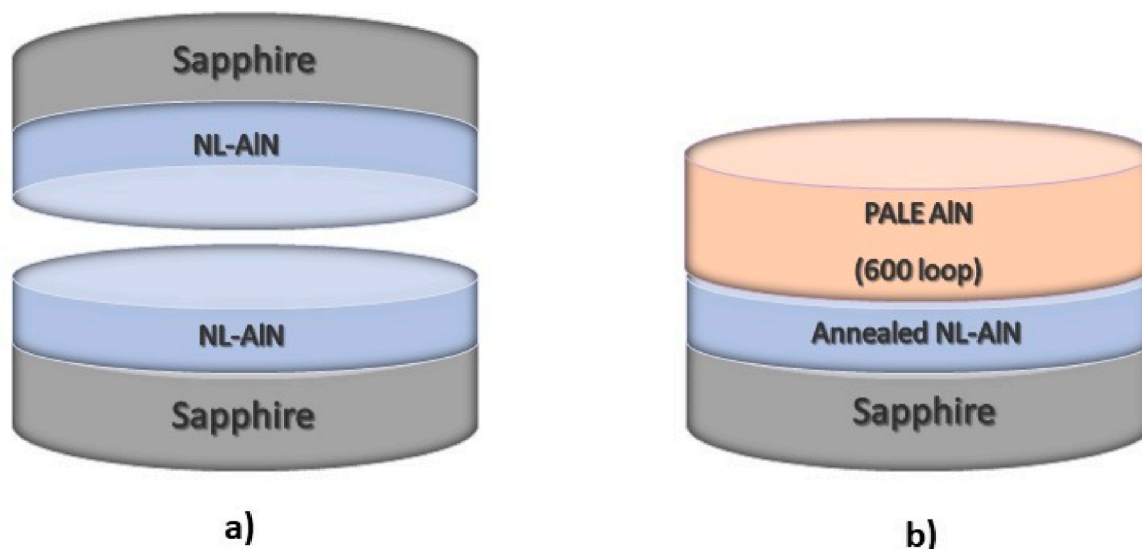


Fig. 1. a) Schematic view of the films during the face-to-face annealing process b) Schematic view of the AlN thin film.

that the NL has a significant effect on the quality and morphology of the AlN film. Therefore, some parameters such as growth pressure, recrystallization temperature, V-III ratio, growth temperature, and time play an important role in the optimization of AlN-NL growth conditions [15].

Annealing is one of the methods used in previous studies to grow AlN films with less threading dislocation densities (TDDs) [16–22]. Annealing energizes the atoms for rearrangement and the grains in the polycrystalline material start to grow and smaller grains can coalesce into larger grains, all of which greatly affect the film quality and property. After NL is annealed, it is transformed into three-dimensional (3D) nucleation island (NIs) [16]. Threading dislocations (TDs) usually occur at the boundaries of NIs. Therefore, the lower density of NIs is beneficial for reducing the TD density in the AlN film during the lateral growth of the islands. It is known that TDs have harmful effects on device performance such as shortening the lifetime of devices [16]. Therefore, the annealing method has been extensively studied in the literature to obtain films with low dislocation density for high-performance devices. Dallaev [23] grown AlN on Si with PE-ALD and then annealed it at

1350 °C in N₂ atmosphere. After annealing, it was observed that the amount of oxygen decreased and the amount of nitrogen increased. This study that annealing has a positive effect on AlN. However, observed that the Si and AlN interfaces were not abrupt after annealing. It has been reported that annealing using a heat resistant substrate will be beneficial for the interface. Miyake et al. [17,18] prevented thermal decomposition of the AlN film during annealing by overlapping the AlN films face-to-face. Lu Zhao et al. [19] studied the annealing process of sputtered AlN films on sapphire substrates with different thicknesses in N₂ ambient. They reported that the crystal quality of AlN films improved significantly after high-temperature annealing (1400–1700 °C). S. Hagedorn et al. [20] investigated the annealing of sputtered (SP) AlN of 350 nm and 450 nm thickness on sapphire in the temperature range of 1650 °C–1730 °C. They reported that the most significant reduction in TDD from $3 \times 10^{10} \text{ cm}^{-2}$ to $4 \times 10^8 \text{ cm}^{-2}$ initially was obtained for 450 nm AlN at an annealing temperature of 1680 °C. Rapid thermal annealing (RTA) is known to be an efficient way to make better the crystalline quality of semiconductors. In III nitride films, it can balance fluctuations of nitrogen concentration and reduce crystal defects [21]. J. C. Zolper et al. [22] showed that rapid thermal annealing performed in Ar or N₂ ambient at 1100 °C improved GaN surface morphology and photoluminescence intensity. As it can be understood from the studies, the optical and surface properties of the materials improved by reducing the defects in the materials with annealing [24].

Although the cost of the annealing process is low and easy to implement, when the studies in the literature are examined, furnace annealing is not practical and cost-effective due to the long annealing time and high temperatures [25]. The ex-situ (RTA) process is remarkable among other annealing methods with its lower transition time, lower crystallization time, and lower cost compared to a furnace and in-situ process for a given annealing temperature. In this current study, the effect of NL annealed at 1100 °C face-to-face in-situ and ex-situ processes on the crystalline, optical, and morphological quality of AlN thin film was investigated for the first time in the literature.

2. Experimentally

AlN thin film samples have been grown on 2-inch c-plane sapphire substrate with AIXTRON 200/4-HT horizontal flow, low-pressure MOVPE system. Firstly, the sapphire substrate has been desorbed at 1245 °C in an H₂ atmosphere for 10 min to remove the water vapor, oxygen, etc. impurities from the surface. The NL is grown at 1080 °C for 5 min using trimethylaluminum (TMAI) metalorganic precursor and

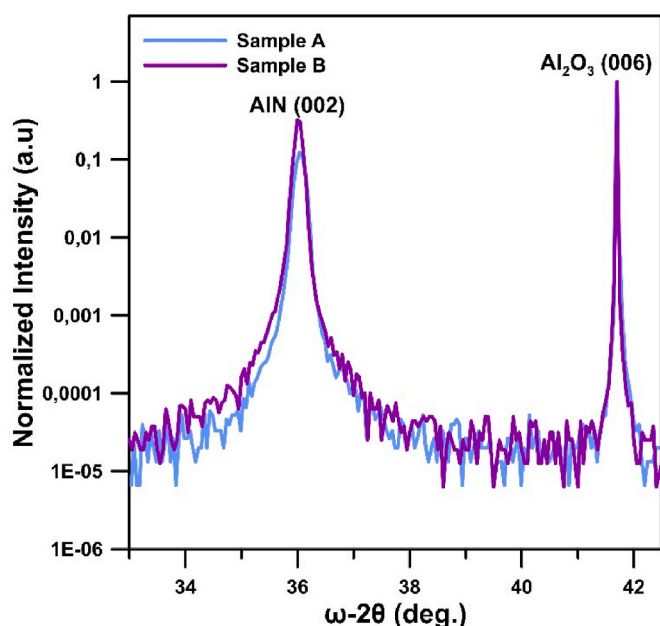


Fig. 2. HRXRD $\omega-2\theta$ scans for Sample A and Sample B.

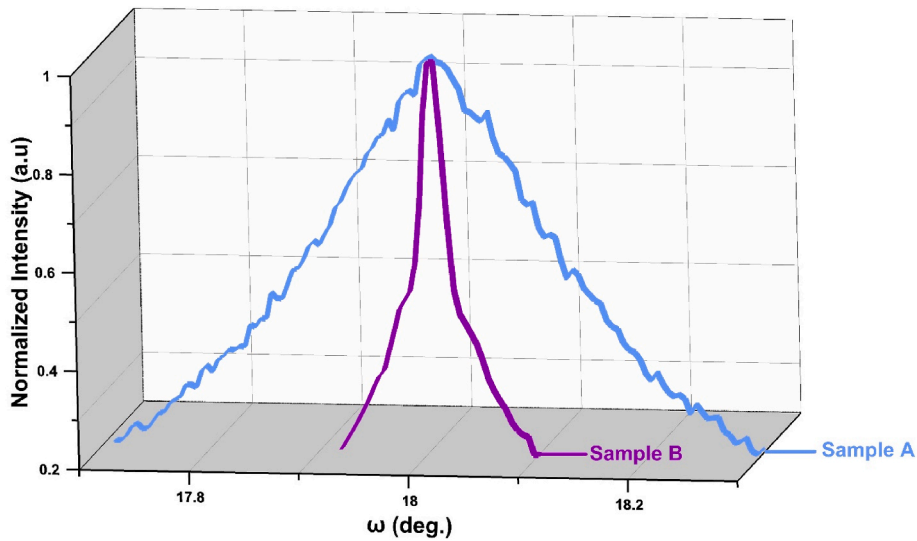


Fig. 3. The comparison of HRXRD ω (002) scans for Sample A and Sample B.

ammonia (NH_3) hydride precursor. After the growth of NL-AlN, the sample has been removed from the reactor and capped with another AlN thin film, and annealed as seen schematically in Fig. 1a. The in-situ process and ex-situ process are named as Sample A and Sample B, respectively. While sample A has been annealed at 1100 °C under N_2 flow in-situ process for 3 h, sample B has been annealed at 1100 °C with a rate of 100 K/s ex-situ process for 180 s under N_2 flow. After annealing of sample A and sample B, high-temperature (HT) AlN layers have been grown on both samples by MOVPE using the pulsed atomic layer epitaxy (PALE) method. The schematic diagram of the grown samples is shown in Fig. 1b. The characterization of the grown samples has been carried out using high-resolution X-ray diffraction (HRXRD), UV-VIS-NIR Spectrophotometer, atomic force microscopy (AFM), and Raman Spectroscopy.

3. Results and discussion

XRD is a well-known technique that is frequently used for the structural properties of thin films [26]. 2Theta/Omega (2θ - ω), symmetric omega (002) and asymmetric omega (102) scans have been carried out to investigate the effect of different annealing processes on crystal quality. Information on the strain and lattice parameters of AlN films has been obtained using ω - 2θ XRD patterns. The peak positions in the XRD patterns are used for strain analysis as shown in Fig. 2. The peak positions of sample A and sample B are 36.1400° and 36.0248°, respectively. Calculated lattice parameter c values of AlN films are given as 4.9817 and 4.9802 Å for Sample A and Sample B, respectively. The lattice parameter $c_0 = 4.978$ Å corresponds to the bulk AlN crystal [27]. The calculated c values for both samples are larger than the

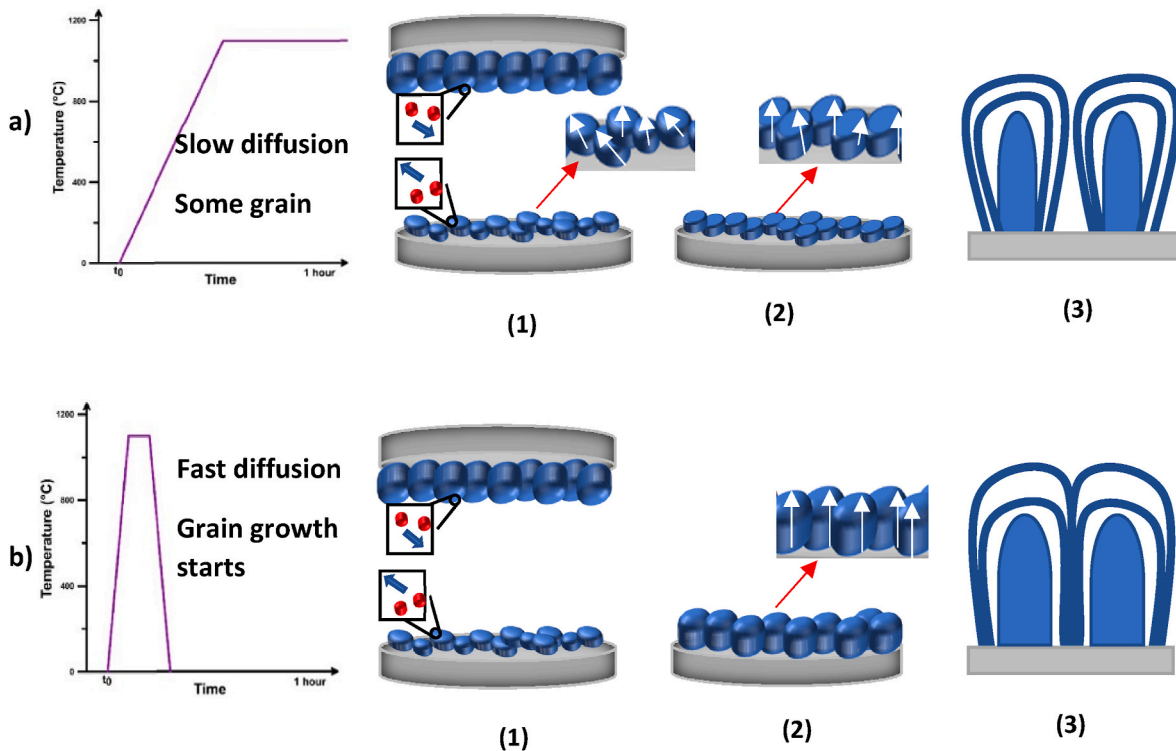


Fig. 4. Schematic representation of a) in-situ process and b) ex-situ (RTA) process methods on the structure (Red circles represent atoms).

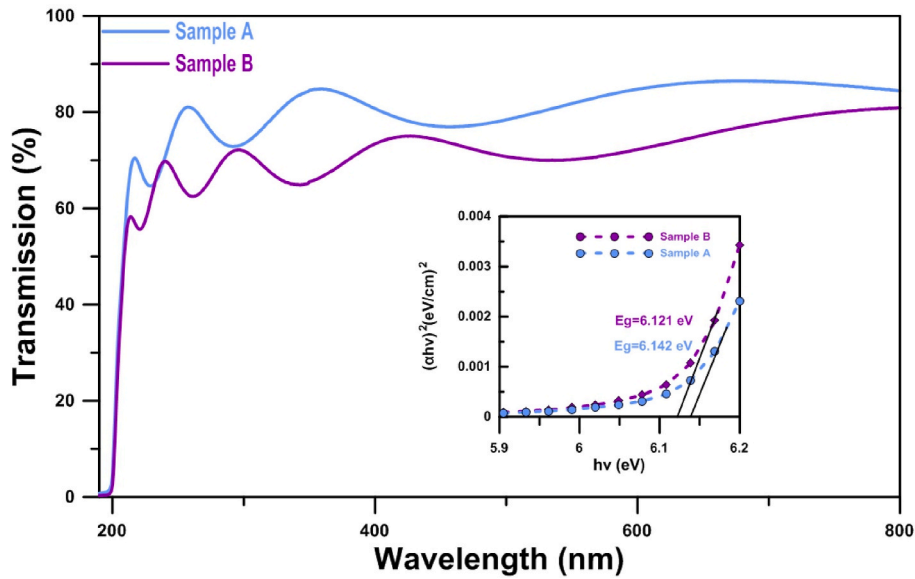


Fig. 5. Transmittance graph of Sample A and Sample B and graph of the photon energy ($h\nu$) versus $(\alpha h\nu)^2$ derived from transmittance measurement.

unstrained c_0 and indicate a tensile strain along the c-axis in the AlN thin films. The tensile strain value for Sample B with a rate of 0.044% is lower than the rate of 0.074% obtained for Sample A.

Furthermore, the crystal quality of the AlN layers has been investigated by using the ω (002) measurement indicated in Fig. 3. The FWHM values obtained for samples A and B are respectively as follows: 700 and 450 arcsec for ω -2 θ scan, 1100 and 200 arcsec for ω (002) scan, 2150 and 1950 arcsec for ω (102) scan. FWHM values are commonly used to calculate dislocations in the AlN epitaxial film [28]. The FWHM values obtained from the ω (002) scan are related to the screw type dislocation density while the FWHM values obtained from the ω (102) scan are related to the edge type dislocation density [27–29]. The screw and edge type dislocation densities of the AlN epitaxial film are calculated using the following equations:

$$D_{\text{screw}} = \frac{\beta_{002}^2}{4.35 b_{\text{screw}}^2} \quad \text{and} \quad D_{\text{edge}} = \frac{\beta_{102}^2}{4.35 b_{\text{edge}}^2}$$

where D_{screw} and D_{edge} are the screw and edge type dislocation density and β_{002} and β_{102} stand for the FWHM values obtained by HRXRD ω scans ((002) and (102)), respectively [30–32]. Also, b_{screw} and b_{edge} correspond to the Burgers vector length ($b_{\text{screw}} = 0.4980$ nm $b_{\text{edge}} = 0.3111$). The D_{screw} values for Sample A and Sample B are 2.64×10^9 (cm^{-2}) and 8.71×10^7 (cm^{-2}), respectively. The D_{edge} values for Sample A and Sample B are 2.58×10^{10} (cm^{-2}), and 2.12×10^{10} (cm^{-2}), respectively.

It can be understood from the measurements and analyses that the crystalline quality of AlN is improved by the ex-situ (RTA) process more than by in-situ process. Higher density threading dislocation has been observed with in-situ process. It is thought that solid-state reaction and recrystallization occur during annealing [17]. Thus, threading dislocations and domain boundaries are diminished. The difference in crystal quality between in-situ process and ex-situ (RTA) process can be attributed to the nucleation sites and subsequent grain size. Fig. 4 shows the schematic diagram of a) in-situ process and b) ex-situ (RTA) process. Fig. 4a(1) and Fig. 4b(1) demonstrate the time (t_0) before annealing. During annealing, AlN decomposition has been prevented with another AlN sample as a face-to-face set up to suppress the thermal decomposition of the AlN films [17]. This technique is known as face-to-face annealing. As seen in Fig. 4a(1) and Fig. 4b(1) in the first step, the grains in the NL have different orientations and are randomly distributed on the surface. In Fig. 4a(2) and Fig. 4b(2), the NL after annealing is

given for the in-situ process and ex-situ (RTA) process. After the ex-situ (RTA) process, the grain size increases with rapid diffusion and grains are high-oriented with c-axis perpendicular to the substrate surface. The films annealed with the UNITEMP RTA-100 system has become a steady-state at 1100 °C within ≈ 1 min with a high increasing rate (100 Ks^{-1}). In this case, the rapid diffusion of Al adatoms has occurred and the nucleation of AlN has begun throughout the film. Thus, a more homogeneous NL and larger particle sizes have been obtained. In-situ process has been stabilized the system for a long time with a slower heating rate. Unlike the ex-situ (RTA) process, relatively small grains with different orientations have been consisted due to the slow diffusion with the in-situ process. In Fig. 4a (3), the larger grains obtained after the ex-situ (RTA) process increase the possibility of coalescence. In Fig. 4b (3), it is more difficult to coalesce because annealing with an in-situ process causes small grains.

The grain sizes have been calculated for both samples from XRD data using Scherrer's equation. The grain sizes of Sample A and Sample B have been calculated as 40.11 nm, and 75.18 nm, respectively. As the grain boundaries have been decreased because of the increase in grain size with ex-situ (RTA), dislocations have been eliminated and crystal quality has improved. These results reveal that the combination of face-to-face and ex-situ (RTA) can be an attractive alternative for AlN template production at lower temperatures and shorter times.

After the in-situ and ex-situ (RTA) processes, the transmittance of the AlN layer has been carried out. The behavior of transmittance for the wavelengths between 200 nm and 800 nm is presented in Fig. 5. The interference patterns observed in the spectra represent the formation of an abrupt interface between AlN thin film and sapphire. Sample A shown a higher transmittance than Sample B. This can be explained as follows: high oxygen concentration in AlN can cause defect complexes that can lead to absorption in the UV range [33]. Since there is a vacuum environment in the reactor during in-situ process, no additional oxygen is added to the structure. However, since there is no vacuum environment in ex-situ (RTA) process, oxygen diffusion into the structure is possible during annealing. Thus, the oxygen concentration in the Sample B is relatively higher than in Sample A, leading to a reduction in transmittance. The optical band gap (E_g) can be estimated by fitting the photon energy ($h\nu$) versus $(\alpha h\nu)^2$ from a Tauc plot to the linear part as shown in Fig. 5. While the E_g value is 6.121 eV for Sample B, it increases to 6.142 eV for Sample A. The increase in the E_g value is thought to be a result of oxygen diffusion, which may be included in the structure during annealing.

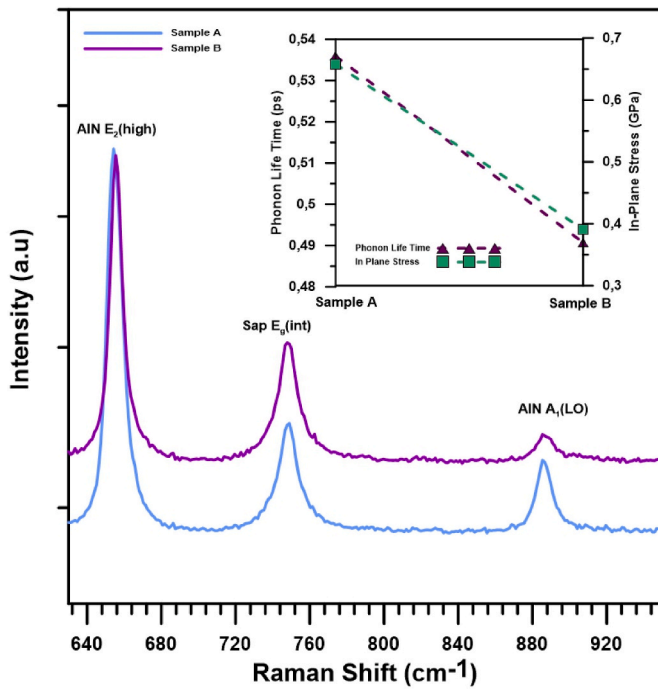


Fig. 6. Raman spectra of Sample A and Sample B and graph of in-plane stress and phonon lifetime derived from Raman spectra.

The Raman spectra of the AlN films have been obtained at a temperature of 300 K in the range of 600–950 nm, as shown in Fig. 6. The allowed E₂ (High) and A₁ (LO) modes have been observed in both samples. The A₁ (LO) phonon mode has been observed at a frequency of

890 cm⁻¹ for both samples. The FWHM value of the A₁ (LO) mode in Sample B is higher than in Sample A. A₁ (LO) phonon mode FWHM value is directly related to film quality. A₁ (LO) phonon lifetime is calculated based on the energy-time uncertainty using the FWHM value, this relationship is given below [34].

$$\frac{\Gamma}{\hbar} = \frac{1}{\tau}$$

where τ is the phonon lifetime (unit is picosecond), \hbar is the modified Planck constant ($5.3 \times 10^{-12} \text{ cm}^{-1} \text{ s}$), and Γ is FWHM (unit cm^{-1}) value. The data of the calculations made using this formula are given in Fig. 6 (inset). It has been observed that Sample B has a short phonon lifetime than Sample A. The short phonon life is suitable for carrier migration, namely shows that the probability of collision with impurities, crystal lattice, etc. decreases during carrier movement.

To investigate the effect of in-situ and ex-situ (RTA) face-to-face annealing on the morphology of AlN thin film, AFM images at $1 \times 1 \mu\text{m}^2$ have been taken. AFM images of Sample A and Sample B face to face annealing are given in Fig. 7. By subjecting the surface reconstruction to the annealing process, it can be concluded that the small grains grow and coalesce into larger grains. Root mean square (RMS) roughness values of Sample A and Sample B have been obtained as 0.184 and 0.256 nm, respectively. As a result of XRD scanning, higher crystal quality has been obtained in Sample B, despite the long time annealing of Sample A. It is thought that the surface quality can be increased by making optimization studies of annealing the NL with RTA [35].

Compare the results obtained from the studies in the literature with the current study and to reveal the differences, the parameters of the AlN annealing studies are given in Table 1. In Refs. [36,37] annealing temperature is high with MOVPE. The FWHM values in Ref. [36] are much smaller than our study and [37]. However, deep surface cracks were observed after annealing in Ref. [36]. These cracks limit the use of AlN as templates. If our study is compared with sputter annealing [17,19],

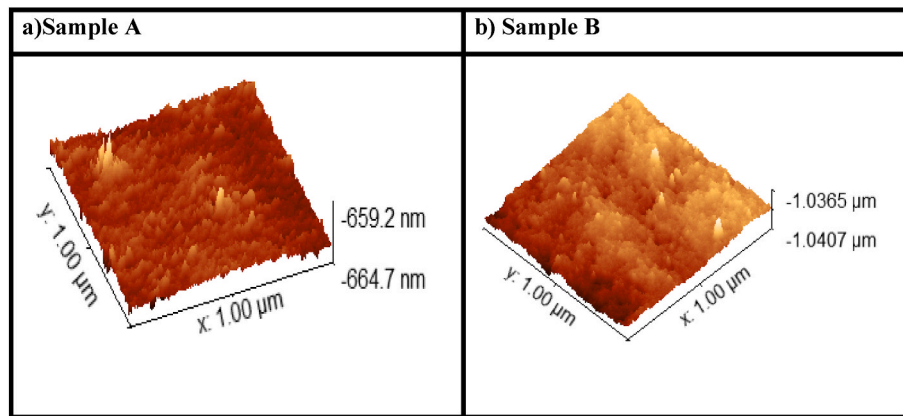


Fig. 7. $1 \times 1 \mu\text{m}^2$ AFM images a) Sample A and b) Sample B.

Table 1
Parameters of annealing studies in the literature.

REF	Thickness	RMS μm^2	FWHM 00.2 (Symmetric)	FWHM 10.2 (Asymmetric)	Annealing Temperature (°C)/Time (h)	Paper Subject
[36]	~350 nm	–	50	450	1700/3	MOVPE annealing
[37]	~555 nm	–	800	1000	1600/1	MOVPE annealing
[38]	~1800 nm	0.42 nm ($1\mu\text{m} \times 1\mu\text{m}$)	610	–	1000/10 s	RTA
[17]	~170 nm	–	49	287	1700/1	Sputter Annealing/Face to Face
[19]	~200 nm	2.10 nm ($2\mu\text{m} \times 2\mu\text{m}$)	103	353	1650/1	Sputter Annealing
Current Study	~200 nm	0.256 nm ($1\mu\text{m} \times 1\mu\text{m}$)	200	1950	1100/3 min	RTA/Face to face
		0.184 nm ($1\mu\text{m} \times 1\mu\text{m}$)	1100	2150	1100/3	MOVPE/Face to face

especially asymmetric (102) FWHM values are lower but RMS value are higher. Although the recrystallization process with the temperature increase reorganized the atoms, the mismatch between the atomic layers was transmitted to the surface layer, thus slightly increasing the surface roughness. FWHM value in Ref. [38] annealed with RTA is higher than our study. One of the issues that should be underlined is to examine the effects of nucleation layer (NL) annealing in our study, while full AlN film annealing is performed in the studies in the literature. Annealing to the nucleation layer is not a common in the literature. Our motivation in this study is to examine different annealing combinations together and to expand the knowledge in the literature with results on how to achieve the required crystal and surface quality without loss of time and material.

4. Conclusions

In our study, the effect of NL annealing with in-situ and ex-situ (RTA) on the properties of AlN thin film has been investigated. The difference in crystal quality seen as a result of annealing with the in-situ and ex-situ (RTA) processes can be attributed to grain orientation and grain size. Thus, if the grain boundaries are reduced, the density of threading dislocations can be decreased. The D_{screw} values calculated from β_{002} for Sample A and Sample B are $2.64 \times 10^9 \text{ (cm}^{-2}\text{)}$ and $8.71 \times 10^7 \text{ (cm}^{-2}\text{)}$, respectively. The D_{edge} values calculated from β_{102} for Sample A and Sample B are $2.58 \times 10^{10} \text{ (cm}^{-2}\text{)}$ and $2.12 \times 10^{10} \text{ (cm}^{-2}\text{)}$, respectively. Examining the spectrophotometer results, Sample A has shown a higher transmittance than Sample B. This can be explained by the high oxygen concentration in AlN causing defect complexes that can lead to absorption. It is seen that the finding obtained from Raman spectrometry and HRXRD measurement are compatible. In-plane strain and stress values have been obtained at a smaller value in Sample B. In the AFM results, it can be concluded that by subjecting the surface reconstruction to the annealing process, the small grains grow and coalesce into larger grains. Root mean square (RMS) roughness values of Sample A and Sample B have been obtained as 0.184 and 0.256, respectively. Although it has better crystal quality, it has been observed that the surface roughness of Sample B is higher than Sample A.

CRedit authorship contribution statement

Merve Nur Koçak: Writing – original draft, Investigation, Conceptualization. **Kağan Murat Pürlü:** Writing – original draft, Investigation, Conceptualization. **İzel Perkitel:** Writing – original draft, Investigation, Conceptualization. **İsmail Altuntaş:** Investigation, Funding acquisition, Formal analysis. **İlkay Demir:** Writing – review & editing, Supervision, Project administration, Methodology, Funding acquisition.

Declaration of competing interest

The authors declare that they have no known competing financial interests or personal relationships that could have appeared to influence the work reported in this paper.

Acknowledgments

The authors acknowledge the usage of the Nanophotonics Research and Application Center at Sivas Cumhuriyet University (CUNAM) facilities. This work is supported by the TUBITAK under Project Number 118F425.

References

- [1] K.M. Pürlü, M.N. Koçak, G. Yolcu, İ. Perkitel, İ. Altuntaş, I. Demir, Growth and characterization of PALE Si-doped AlN on sapphire substrate by MOVPE, *Mater. Sci. Semicond. Process.* 142 (2022), 106464.
- [2] Y. Koçak Demir, A.E. Kasapoğlu, M. Razeghi, E. Gür, &S. Elagoz, GaN/AlN MOVPE heteroepitaxy: pulsed co-doping SiH₄ and TMin, *Semicond. Sci. Technol.* 34 (2019), 075028, 7.
- [3] D. Chen, J. Wang, D. Xu, Y. Zhang, The influence of defects and impurities in polycrystalline AlN films on the violet and blue photoluminescence, *Vacuum* 83 (5) (2009) 865–868.
- [4] İ. DEMİR, Growth temperature dependency of high Al content AlGaIn epilayers on AlN/Al₂O₃ templates, *Cumhuriyet Science Journal* 39 (3) (2018) 728–733.
- [5] H. Kim, N. Do Kim, S.C. An, H.J. Yoon, B.J. Choi, Improved interfacial properties of thermal atomic layer deposited AlN on GaN, *Vacuum* 159 (2019) 379–381.
- [6] D. Cao, X. Cheng, Y.-H. Xie, L. Zheng, Z. Wang, X. Yu, J. Wang, D. Shen, Y. Yu, Effects of rapid thermal annealing on the properties of AlN films deposited by PEALD on AlGaIn/GaN heterostructures, *RSC Adv.* 5 (2015) 37881–37886.
- [7] L. Kolaklieva, V. Chitanov, A. Szekeres, K. Antonova, P. Terziyska, Z. Fogarassy, P. Petrik, I.N. Mihailescu, L. Duta, Pulsed laser deposition of aluminum nitride films: correlation between mechanical, optical, and structural properties, *Coatings* 9 (2019) 195.
- [8] T. Kumada, M. Ohtsuka, H. Fukuyama, Influence of substrate temperature on the crystalline quality of AlN layers deposited by RF reactive magnetron sputtering, *AIP Adv.* 5 (2015), 017136.
- [9] Q. Paduano, D. Weyburne, Two-step process for the metalorganic chemical vapor deposition growth of high quality AlN films on sapphire, *Jpn. J. Appl. Phys.* 42 (2003) 1590.
- [10] X. Rong, X. Wang, G. Chen, J. Pan, P. Wang, H. Liu, F. Xu, P. Tan, B. Shen, Residual stress in AlN films grown on sapphire substrates by molecular beam epitaxy, *Superlattice. Microsc.* 93 (2016) 27–31.
- [11] İ. Perkitel, İ. Altuntaş, İ. Demir, The Effect of Si (111) Substrate Surface Cleaning on Growth Rate and Crystal Quality of MOVPE Grown AlN, *Gazi University Journal of Science*, 1-1.
- [12] İ. Demir, Y. Robin, R. McClintock, S. Elagoz, K. Zekentes, M. Razeghi, Direct growth of thick AlN layers on nanopatterned Si substrates by cantilever epitaxy, *Phys. Status Solidi* 214 (2017), 1600363.
- [13] Altuntas Kocak, G. Yolcu, H.F. Budak, A.E. Kasapoğlu, S. Horoz, E. Gür, I. Demir, Influence of the PALE growth temperature on quality of MOVPE grown AlN/Si (111), *Mater. Sci. Semicond. Process.* 127 (2021), 105733.
- [14] H. Li Demir, Y. Robin, R. McClintock, S. Elagoz, &M. Razeghi, Sandwich method to grow high quality AlN by MOCVD, *J. Phys. Appl. Phys.* 51 (2018), 085104, 8.
- [15] W. Luo, L. Li, Z. Li, Q. Yang, D. Zhang, X. Dong, D. Peng, L. Pan, C. Li, B. Liu, Influence of the nucleation layer morphology on the structural property of AlN films grown on c-plane sapphire by MOCVD, *J. Alloys Compd.* 697 (2017) 262–267.
- [16] L. Shang, B. Xu, S. Ma, Q. Liu, H. Ouyang, H. Shan, X. Hao, B. Han, The surface morphology evolution of GaN nucleation layer during annealing and its influence on the crystal quality of GaN films, *Coatings* 11 (2021) 188.
- [17] H. Miyake, C.-H. Lin, K. Tokoro, K. Hiramatsu, Preparation of high-quality AlN on sapphire by high-temperature face-to-face annealing, *J. Cryst. Growth* 456 (2016) 155–159.
- [18] K. Uesugi, H. Miyake, Fabrication of AlN templates by high-temperature face-to-face annealing for deep UV LEDs, *Jpn. J. Appl. Phys.* 60 (12) (2021), 120502.
- [19] L. Zhao, K. Yang, Y. Ai, L. Zhang, X. Niu, H. Lv, Y. Zhang, Crystal quality improvement of sputtered AlN film on sapphire substrate by high-temperature annealing, *J. Mater. Sci. Mater. Electron.* 29 (2018) 13766–13773.
- [20] S. Hagedorn, S. Walde, A. Mogilatenko, M. Weyers, L. Cancellara, M. Albrecht, D. Jaeger, Stabilization of sputtered AlN/sapphire templates during high temperature annealing, *J. Cryst. Growth* 512 (2019) 142–146.
- [21] D. Cao, X. Cheng, Y.-H. Xie, L. Zheng, Z. Wang, X. Yu, J. Wang, D. Shen, Y. Yu, Effects of rapid thermal annealing on the properties of AlN films deposited by PEALD on AlGaIn/GaN heterostructures, *RSC Adv.* 5 (2015) 37881–37886.
- [22] J. Zolper, M. Hagerott Crawford, A. Howard, J. Ramer, S. Hersee, Morphology and photoluminescence improvements from high-temperature rapid thermal annealing of GaN, *Appl. Phys. Lett.* 68 (1996) 200–202.
- [23] R. Dallaev, Investigation of hydrogen impurities in PE-ALD AlN thin films by IBA methods, *Vacuum* 193 (2021), 110533.
- [24] E. Erdoğan, TVA ile üretilen cam/GaN/inGaIn filmin artan tavlama sıcaklığının bazı fiziksel özelliklerine etkileri, *Erzincan Üniversitesi Fen Bilimleri Enstitüsü Dergisi*, 13 1-10.
- [25] M. Wang, F. Xu, J. Wang, N. Xie, Y. Sun, B. Liu, J. Lang, N. Zhang, W. Ge, X. Kang, The sapphire substrate pretreatment effects on high-temperature annealed AlN templates in deep ultraviolet light emitting diodes, *CrystEngComm* 21 (2019) 4632–4636.
- [26] S. Elagoz, İ. Demir, Growth of InGaAs/InAlAs superlattices by MOCVD and precise thickness determination via HRXRD, *Gazi University Journal of Science* 29 (2016) 947–951.
- [27] D. Nilsson, E. Janzén, A. Kakanakova-Georgieva, Lattice parameters of AlN bulk, homoepitaxial and heteroepitaxial material, *J. Phys. Appl. Phys.* 49 (2016), 175108.
- [28] G. Yolcu Simsek, M. Koçak, K. Pürlü, İ. Altuntas, I. Demir, Nucleation layer temperature effect on AlN epitaxial layers grown by metalorganic vapour phase epitaxy, *J. Mater. Sci. Mater. Electron.* 32 (2021) 25507–25515.
- [29] I. Demir Altuntas, A.E. Kasapoğlu, S. Mobbakeri, E. Gür, S. Elagoz, The effects of two-stage HT-GaN growth with different V/III ratios during 3D–2D transition, *J. Phys. Appl. Phys.* 51 (2017), 035105.
- [30] Z. Su, R. Kong, X. Hu, Y. Song, Z. Deng, Y. Jiang, H. Chen, Effect of initial condition on the quality of GaN film and AlGaIn/GaN heterojunction grown on flat sapphire substrate with ex-situ sputtered AlN by MOCVD, *Vacuum* 201 (2022), 111063.

- [31] J. Luo, W. Wang, Y. Zheng, X. Li, G. Li, AlN/nitrided sapphire and AlN/non-nitrided sapphire hetero-structures epitaxially grown by pulsed laser deposition: a comparative study, *Vacuum* 143 (2017) 241–244.
- [32] Y. Li, X. Hu, Y. Song, Z. Su, W. Wang, H. Jia, H. Chen, Epitaxy N-polar GaN on vicinal Sapphire substrate by MOCVD, *Vacuum* 189 (2021), 110173.
- [33] Q. Yan, A. Janotti, M. Scheffler, C.G. Van de Walle, Origins of optical absorption and emission lines in AlN, *Appl. Phys. Lett.* 105 (2014), 111104.
- [34] L. Bergman, D. Alexson, P.L. Murphy, R.J. Nemanich, M. Dutta, M.A. Stroscio, C. Balkas, H. Shin, R.F. Davis, Raman analysis of phonon lifetimes in AlN and GaN of wurtzite structure, *Phys. Rev. B* 59 (1999), 12977.
- [35] E. Herth, D. Fall, J.-Y. Rauch, V. Mourtalier, G. Guisbiers, Thermal annealing of AlN films for piezoelectric applications, *J. Mater. Sci. Mater. Electron.* 31 (2020) 4473–4478.
- [36] S. Walde, S. Hagedorn, M. Weyers, Impact of intermediate high temperature annealing on the properties of AlN/sapphire templates grown by metalorganic vapor phase epitaxy, *Jpn. J. Appl. Phys.* 58 (SC) (2019) SC1002.
- [37] D.V. Dinh, H. Amano, M. Pristovsek, MOCVD growth and high-temperature annealing of (101 0) AlN layers on (101 0) sapphire, *J. Cryst. Growth* 502 (2018) 14–18.
- [38] B. Liu, J. Gao, K.M. Wu, C. Liu, Preparation and rapid thermal annealing of AlN thin films grown by molecular beam epitaxy, *Solid State Commun.* 149 (17–18) (2009) 715–717.